Proceedings World Geothermal Congress 2026
Calgary, Canada, June 8 – 11, 2026

GEOTHERMAL PROSPECTING OF THE APACHETA GEOTHERMAL FIELD IN BOLIVIA USING 1D INVERSION OF MAGNETOTELLURIC DATA

Oscar Cahuana Alarcon[1]*
Empresa Nacional de Electricidad - ENDE*
*oscar.cahuana@ende.bo; os.cahuana.alarcon@gmail.com

Keywords: Apacheta, Sol de Mañana, geothermal, ENDE, Bolivia, geophysics, magnetotelluric

ABSTRACT

The mineralogy of the wells is playing a very important role in understanding and correlates somewhat with the results of the 1D resistivity model, which was derived from a 1D inversion of magnetotelluric (MT) data with available information for the Apacheta geothermal field, part of the Laguna Colorada area in the southwest of Bolivia, next to Sol de Mañana. The resistivity structure found is characterized by a shallow low-resistivity clay cap oriented approximately east-west along the drilled wells in Sol de Mañana, extending west to the Apacheta geothermal field. Furthermore, two up-doming features are observed beneath both the Sol de Mañana and Apacheta geothermal fields. To confirm the up-doming feature under Apacheta, more soundings are needed around the field.

1 INTRODUCTION

Geothermal research in Bolivia started in the 1970s and Bolivia is developing the use of geothermal sources for different sort of utilization. Carrasco (1976) observed that Bolivia has numerous geothermal surface manifestations in the western Andean region and in other areas of geothermal interest such as the southern area of the western Andean Mountain range (Lípez Province, Department of Potosi), the rims of the central Altiplano (Poopo and Avaroa Provinces, Department of Oruro), and the Chaqui zone (Saavedra Province, Department of Potosi). In 1965 (Waring, 1965) more than 70 areas were mapped with geothermal manifestations, including hot pools, mud pools, fumaroles, and steaming ground. Also, Donovan (1984) listed Bolivia, as a country with number of prospects where geothermal reconnaissance studies have indicated areas for pre-feasibility studies, concluding that the geothermal potential of Bolivia is significant.

Gawell et al. (1999) reported a geothermal potential for Bolivia between 510 MWe and 1260 MWe and with enhanced geothermal systems this potential will increase between 1070 MWe and 2490 MWe. Also, as Bolivia is a natural gas and oil producer, it has a several closed wells in possible low-grade geothermal sites, so according to recent research, regions of extensive hydrocarbon exploration are often close to market and with significant geothermal gradients (Santos et al, 2022).

Due to these facts, since 1976, Empresa Nacional de Electricidad (ENDE), which is a state-owned company, with the support of United Nations Development Programme (UNDP) and Italy's government determined the areas of Laguna Colorada, Sajama Volcano and Empexa Valley as the most promising sites for resource exploration geothermal (Battocletti and Lawrence, 1999; Delgadillo, 2000).

Subsequently, between 1978 and 1980, ENDE carried out pre-feasibility studies in the areas of Laguna Colorada and Empexa Valley, identifying great potential in the Sol de Mañana sector of the Laguna Colorada area. From that moment on, geothermal activity in Bolivia was concentrated on Sol de Mañana field. In 1985, ENDE began a feasibility study in collaboration with the Entity National Electricity of Italy – ENEL, AQUATER (an Italian consulting company) and Yacimientos Petrolíferos Fiscales Bolivianos (YPFB) (oil Bolivian state-owned), which made the drilling equipment available. Between 1988 and 1992 six wells were drilled to an average depth of 1500 meters, confirming the existence of an important high temperature geothermal resource (Delgadillo, 2000; Villarroel, 2014). Owing to political issues in 1993, Laguna Colorada project was suspended (Battocletti and Lawrence, 1999).

To continue with Laguna Colorada project, between 1996 and 1997, ENDE hired to Comisión Federal de Electricidad de México (CFE) to evaluate and certify the potential resource. The results of the evaluation of the CFE had two scenarios; 1) generation of 120 MWe with two plants of 60 MWe and 2) generation of 240 MWe with four 60 MWe plants (CFE, 1997; Delgadillo, 2000). By 2008, Japan External Trade Organization – JETRO confirmed the viability of a 100 MWe commercial development over 30 years (JETRO, 2008). Based on these results, the

Cahuana O.

Japan International Cooperation Agency (JICA) and government of Bolivia began discussions in 2010 on the financing of the building of a 50 MWe geothermal power plant at Sol de Mañana field. In July 2014, the Government of Bolivia signed a loan contract with JICA to be executed by ENDE. During phase zero of the project, the installation of a 5 MWe pilot plant is planned. (ENDE, 2017).

Consequently, in December 2018, ENDE signed a contract with the joint venture Sacyr-Ormat for designing and installation of a binary technology plant in Sol de Mañana field. The power plant will sit at 4.970 m and thereby be the power plant at the highest elevation in the world. The aim is to evaluate the technology for developing a plant of 100 MWe and direct the electricity to population near to it. This project is underway

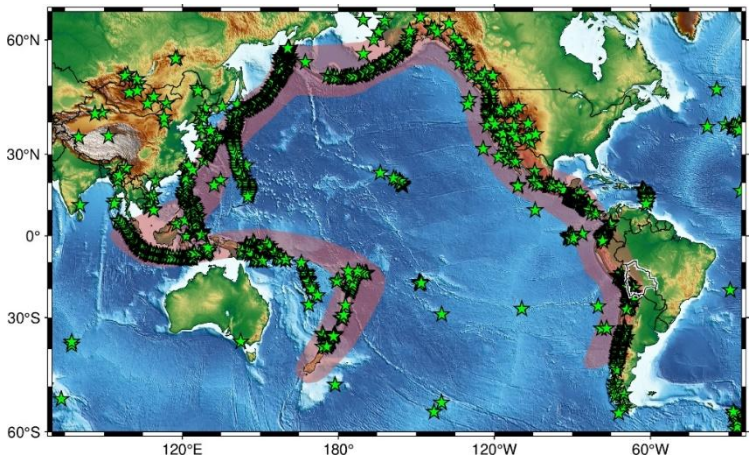
2 GEOLOGICAL SETTINGS

2.1 REGIONAL GEOLOGY

One of the major volcanic areas in the world is the Andean Volcanic Belt (part of the Ring of Fire, see Figure 1), hosts four active volcanic zones: Northern, Central, Southern and Austral. The Central Volcanic Zone of the Andes (CVZ) extends from southern Peru in the south, north through western Bolivia, north-western Argentina, and northern Chile. CVZ forms the western boundary of the Altiplano plateau. This volcanic arc developed due to the subduction of the Nazca plate under western South America plate.

The CVZ has six potentially active large silicic volcanic systems: Altiplano-Puno Volcanic Complex, Cerro Panizos, Pastos Grandes, Cerro Guacha, La Pacana and Los Frailes (Aguilera, 2021; DeSilva, 1989) (See Figure 1). The part of the CVZ in Bolivia is divided into two volcanic complexes, Cordillera Occidental in the west (Western Cordillera) and Cordillera Oriental in the east (Eastern Cordillera) (See Figure 2A). Cordillera Occidental makes up the natural border with Chile, and the Cordillera Oriental extends south-eastward. Figure 2A shows the surface geothermal manifestations in Bolivia from Waring (1965), Carrasco (1976) and Aliaga (1985). Most of the surface manifestations (red in Figure 2A) are between Western and Eastern Cordilleras, along the Altiplano. Other surface manifestations are showed in green in Figure 4A, those were reported by local people (Salas, 2014) in recent years. Some of the surface manifestations utilized by people as swimming pools.

The concession area of Laguna Colorada (purple line in Figure 2B) is in the Miocene-Pleistocene part of the CVZ, which extends in north-south direction over the Western Cordillera. The volcanic products are overlain by sediments of mesozoic and paleogene age. The mineral products of the volcanic arc have a composition of calcium-alkaline, varying between andesite and hydrocite,



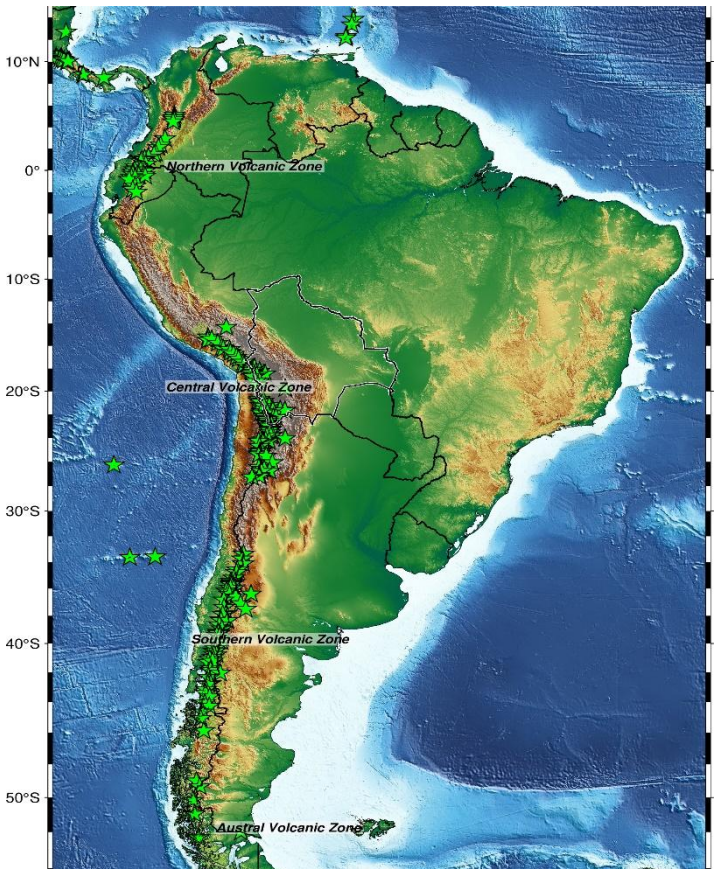


Figure 1. Top: The Ring of Fire in red shadow. Bottom: The Andean Volcanic Belt. Green stars represent volcanoes.

consisting of lavas and ignimbrites (JETRO, 2008).

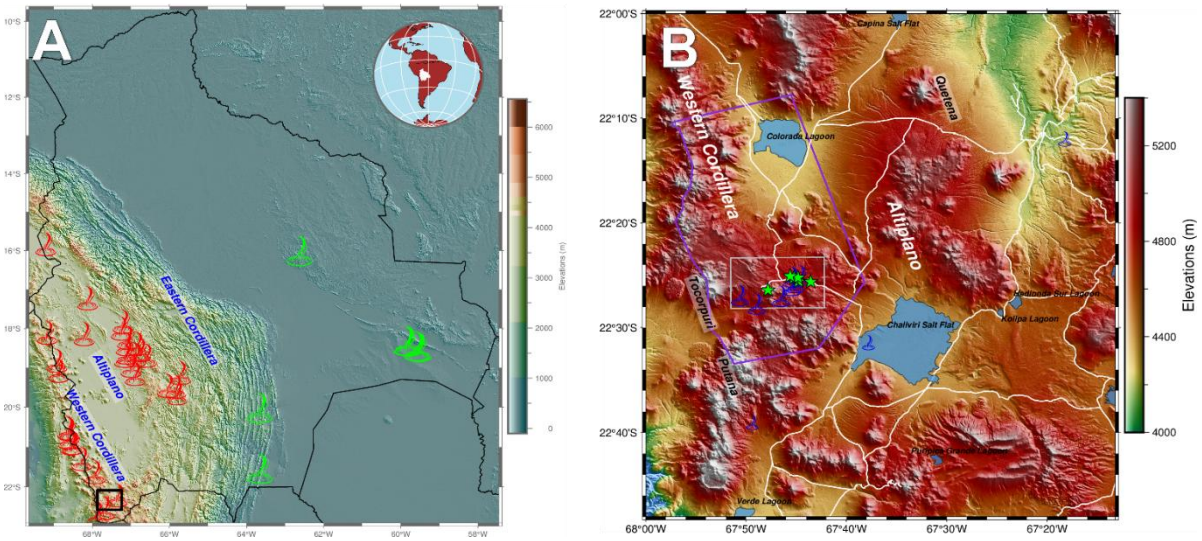


Figure 2. A. Surface manifestations in Bolivia. Surface manifestations are located in the Altiplano (red) and in eastern Bolivia (green). A global Earth relief grids with 3 arc seconds accuracy was used (Tozer et al., 2019). The upper right corner shows the location of Bolivia. Black box shows the study area and thin black lines are international borders. B. Study area, located in the flat part of the Altiplano, just in the foothills of the Western Cordillera. Blue icons show the surface manifestations, green stars are drilled wells, purple polygon is Laguna Colorada area and grey box is the study area for this report.

2.2 LOCAL GEOLOGY

The location of Sol de Mañana and Apacheta fields (Figure 2B) is between the Western Cordillera and the Altiplano-Puna plateau (this last is most know in Bolivia just as Altiplano). The area has an intense volcanic activity since 23 Ma with a production of acid magma, characterized by powerful ignimbrite and andesitic lava flows. The elevation of the study area is 4900 meters above sea level (m.a.s.l.).

To date, six wells have been drilled in the study area, five in the Sol de Mañana (wells SM 1-5) field and one in the Apacheta field (AP-1 well), which is our study focus. Figure 3 shows two tectonic fault systems, the first is the set of main faults extending in WNW-ESE direction (black lines) and the second set in NE-SW direction (gray lines). Most WNW-ESE faults are over Sol de Mañana wells and some of them close to AP-1 well, most likely control fluid flow and distribution of geothermal fluid. This assumption will be explained in the Section 5 of this report.

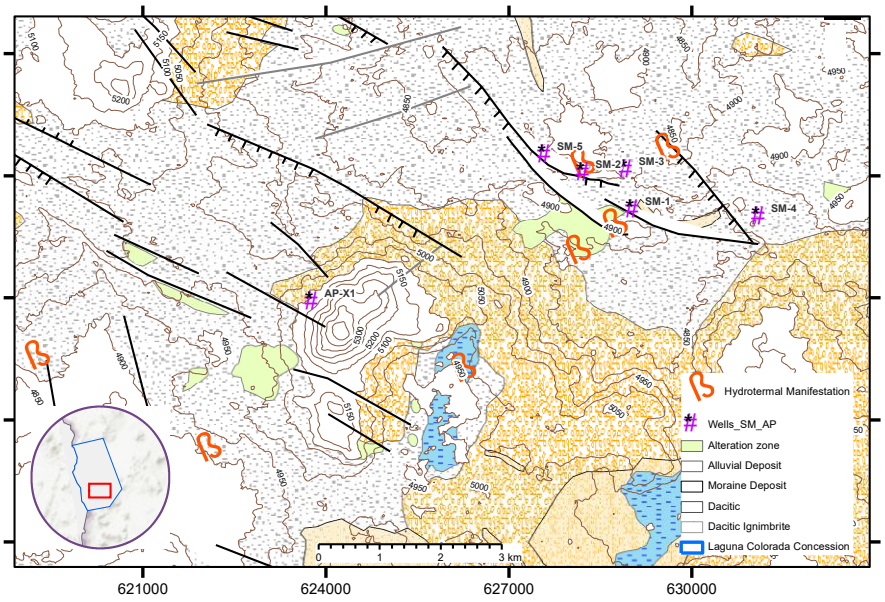


Figure 3. Geological map of Sol de Mañana and Apacheta geothermal fields. Purple triangles are the wells. Black and gray lines are the faults.

2.2.1 LITHOLOGY

The volcanological distribution of the Laguna Colorada field indicates the existence of a large unit of ignimbrite, which almost covers the entire area and overlaps a sequence of andesite-dacite lava of neogeogenic age (see Figure 3). It is worth mentioning that Cerro Apacheta unit appears in the lithology from well of AP-1 and extends towards to the border with Chile and disappears around the wells of SM field. This Apacheta unit is an important layer in El Tatio and La Torta, geothermal fields located in Chile, around 20 km west and north of our study area, respectively (Piscaglia, 2012; Urzua, 2002).

2.2.2 MINERALOGY

The appearance of hydrothermal alteration minerals is used as a past or present indicator of temperature and for estimates of the cap rock layer. The minerals observed in Sol de Mañana field are clay, silicas, zeolite, lamonite, cericite, chlorite, calcium, pyrite, and epidote. Three alteration zones in the local wells are defined based on their mineralogical association (see Figure 4):

- Argilic alteration zone: characteristic by clay, silicate, zeolites that correspond to temperatures less than 180 °C, it extends to a depth of 500 meters. But in the SM-4 well this zone lies deeper than in the other wells. The clay cap starts in this layer.

- Silicified alteration zone: with abundant silica associated and mixed with silicates and chlorites that determine a temperature between 180 °C and 220 °C. The zone extends to a depth between 700 m and 800 m in SM-1, SM-2, SM-3, at 1000 m in SM-5 and AP-1, and more than 1300 m in SM-4. During drilling this zone showed little sign of water losses and the temperatures in the zone were high, suggesting that this zone corresponds to part of the clay cap (cap rock).

- Epidote zone: characteristic by chlorite, silica, albite, and adularia. The temperate in this zone is more than 200 °C and it extends to the bottom of the wells. Feed zones are present in this layer.

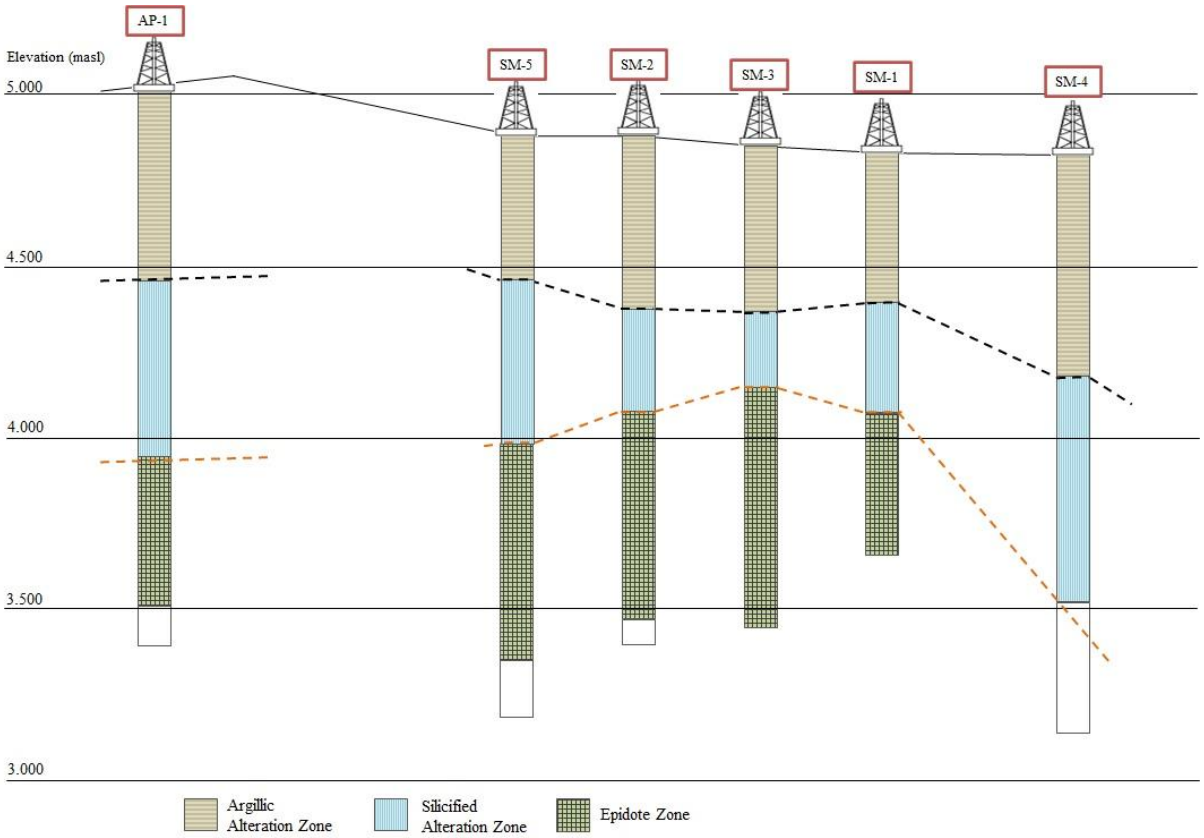


Figure 4. Alteration minerology in the six different wells in the Sol de Mañana and Apacheta fields

3 GEOPHYSICAL EXPLORATION

4 MAGNETOTELLURIC METHOD IN LAGUNA COLORADA AREA

The MT data in the Sol de Mañana and Apacheta geothermal fields were collected by company Teranov Geothermal Energy and CGG was subcontracted for final processing. Figures 5 and 6 show the location of the 70 MT soundings that were acquired. The stations collected data for 17 hours. A remote station collected data during the project time, located 35 km from the survey area (green triangle in Figure 5). This site was chosen because the topography is relatively flat, there is not much wind because of mountains in the western part. Also, it is far away from touristic paths, and it has porty vegetation, so the animals have not been considered a problem. The following sources were considered as noise sources in the MT survey: borax factory (it has a power generator working all day), tourist and animal activities, and wind ´s effect.

4.1 DATA ACQUISITION

The setup of each MT station was relative towards geographical north. A compass was used for orientation and the level of the magnetic coils was verified using a bubble level. The dipoles measure 100 m at all sites, except for site 75 where the length was 98 m. Five Metronix data loggers ADU07e and fifteen induction coil magnetometers were used. Five channels were recorded at each station: E_x, E_y, H_x, H_y and H_z.

4.2 DATA PROCESSING

The surveyor for Laguna Colorada project pre-processed the raw data (time-series). Five files were acquired at each site (4096 Hz Low Gain, 4096 Hz High Gain, 2048 Hz y 128 Hz). The on-site surveyor processed the data using Mapros software where the data were converted from the time domain to the frequency domain (from *.ats to *.edi).

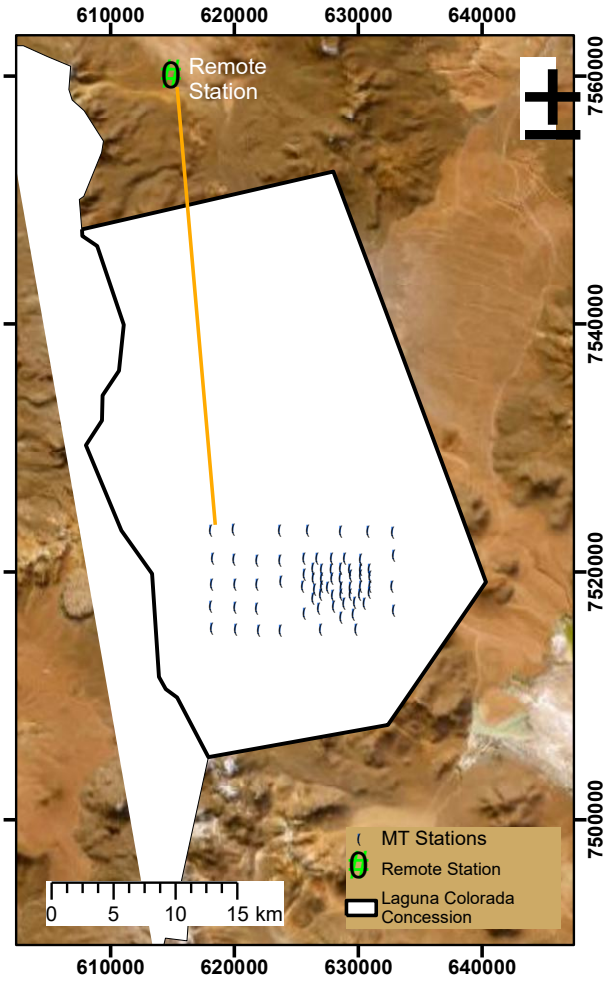


Figure 5. Laguna Colorada concession (black polygon) and the MT stations collected at Sol de Mañana and Apacheta fields.

The data are of very good quality in most of the stations. 65 out of 70 stations were used in the 1D inversion (See Figure 6). Figure 7 shows an example of different parameters that are obtained from the MT soundings. These include apparent resistivity and phase from the xy and yx components of the impedance tensor (red and blue data, respectively in Figure 7). In Figures 7 and 8 the determinant invariant is shown in black. Figure 7 also shows parameters as Zstrike and Tipper, this last is related to the local vertical magnetic field.

A skew angle is a parameter that describes the dimensionality of the MT data. Skew values between 0.1-0.3 are considered 2D distorted and values less than 0.1 are considered for 1D or 2D (Swift, 1967; Bahr 1991). Skew values close to 0 indicate a 1D Earth. Many of the soundings have values of skew close to 0 for periods <10s, making them ideal for 1D inversion. The skew parameter increases in many cases to larger than 0.1 and 0.3 at longer periods, indicating a 2D or 3D structure. Moreover, this characteristic is also founded in the data collected from MT survey made in the south part of Bolivia and north of Chile and Argentina, carried out by the project called PLUTONS (Corneau, 2015).

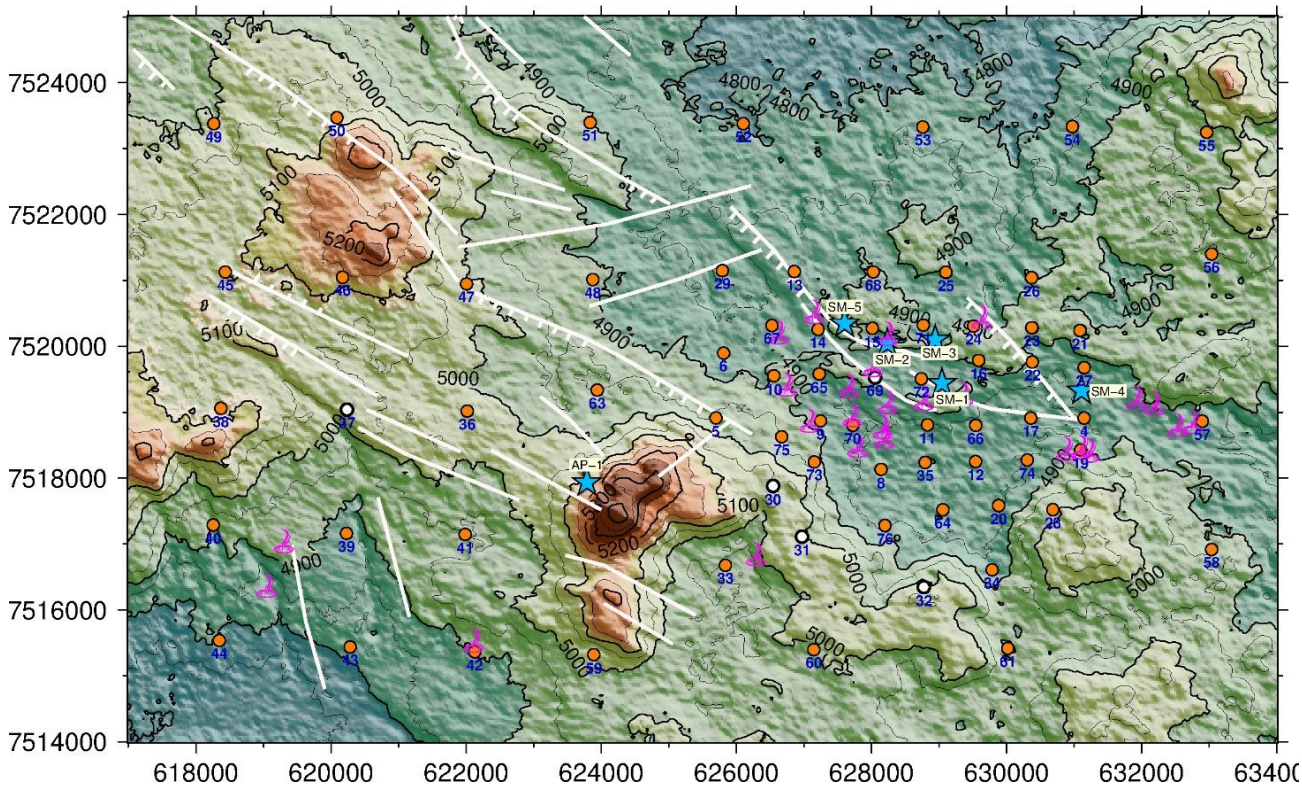


Figure 6. Location of MT stations. Orange circles represent soundings used in the 1D inversion; white circles were not used due to bad quality; blue stars are wells and surface manifestations are in violet. Recent surface manifestations found in Pereyra (2023) are shown. White lines are faults and fractures. Coordinates of soundings are detailed in Appendix I in Cahuana, 2023.

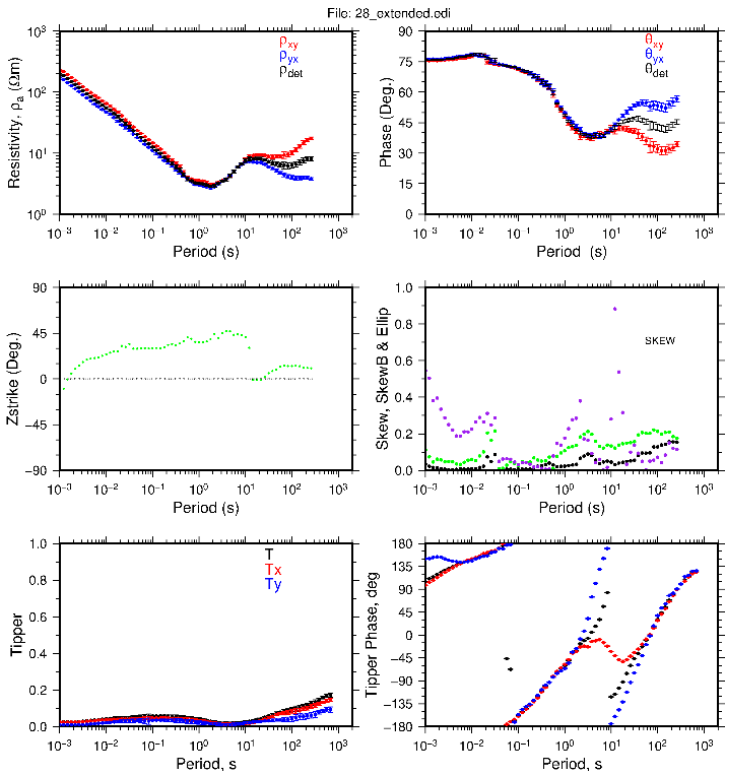


Figure 7. Processed MT data for sounding 28. All results are in Appendix II in Cahuana

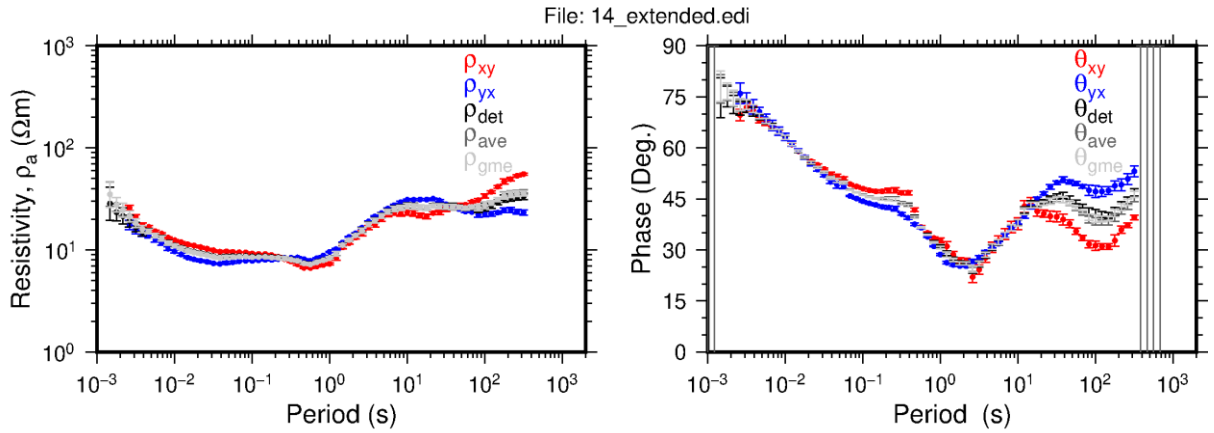


Figure 8. Processed MT data for sounding 14. All the invariant parameters are similar, but note how the average (arithmetic mean) deviates for periods higher than 300 s.

4.3 1D OCCAM'S INVERSION

The program TEMTD was used to perform 1D inversion of MT data. TEMTD was written by Árnason (2006b) in ANSI-C programming language and runs under UNIX/LINUX operating systems, it uses the gnuplot graphics program for graphical display during the inversion process. As the inversion is 1D the Earth is assumed to be layered. The program can invert for only TEM or MT data and for joint inversion of TEM and MT data. Laguna Colorada project just has MT.

The forward algorithm for MT is the standard complex impedance 1D recursion algorithm. The inversion algorithm used in TEMTD is based on the Levenberg-Marquardt non-linear least square inversion as described by Árnason (1989). The program solves for resistivities and thicknesses of discrete layers and uses both amplitude and phase as input. During inversion, the program offers the possibility to keep models smooth with respect to resistivity variations between layers and layer thicknesses. Moreover, it provides options for applying a damping factor which counteracts sharp steps and oscillations in the model values. The function that is minimized is the potential given by the equation below:

$$Pot = chisq + \alpha * DS1 + \beta * DS2 + \gamma * DD1 + \delta * DD2 \quad (1)$$

Where DS1 and DS2 = first and second order derivatives of log-conductivities in the layered model;
DD1 and DD2 = first and second order derivatives of the logarithms of the ratios of layer depths;
$\alpha, \beta, \gamma, \delta$ = coefficients of the different damping terms.

The programme can perform minimum structure (Occam's) inversion. In this case the layer thicknesses are kept fixed, equally spaced on log scale, and the conductivity distribution is forced to be smooth by adjusting α and β in the potential above (the damping of variation of layer thicknesses is of course ignored in this case).

During the 1D inversion, the average thickness of the first layer was 42 m and was given a constant resistivity value between 10 and 140 Ωm. All the inversions ran with 30 layers. It is important to mention that the factor to scale large uncertainties to equalise data weights was fixed in 0.9 as with this value it a good fit was obtained. The minimum percent uncertainty was between 3 and 9. The misfit of the model was evaluated by the chi-square parameter, and most errors were less than 1. The static shift multiplier was not used in the beginning, but for some stations it was necessary to use it to get a consistent resistivity model. Figure 9 shows an example of the 1D inversion (See Appendix II in Cahuana, 2023 for all the results).

No co-located TEM soundings were available, so the low-resistivity cap was assumed to be un-broken in the 1D resistivity model. To maintain that assumption, it was necessary to apply the shift multiplier at 6 stations. There are different causes for the static shift phenomena, and one is the presence of shallow resistivity heterogeneities close to the sounding site (Árnason, 2015). On a log-log plot of apparent resistivity versus frequency the shape of the apparent resistivity curve remains unchanged because the distortion is frequency independent, but the curve may be vertically translated (or shifted) (see Figure 10) since the apparent resistivities (y-axis) are scaled by the static shift coefficient. However, the phase remains unaffected (See Figure 10), as do the induction

vectors (Jones and Groom, 1993). If the static shift is not corrected the inversion models may be interpreted in a wrong way.

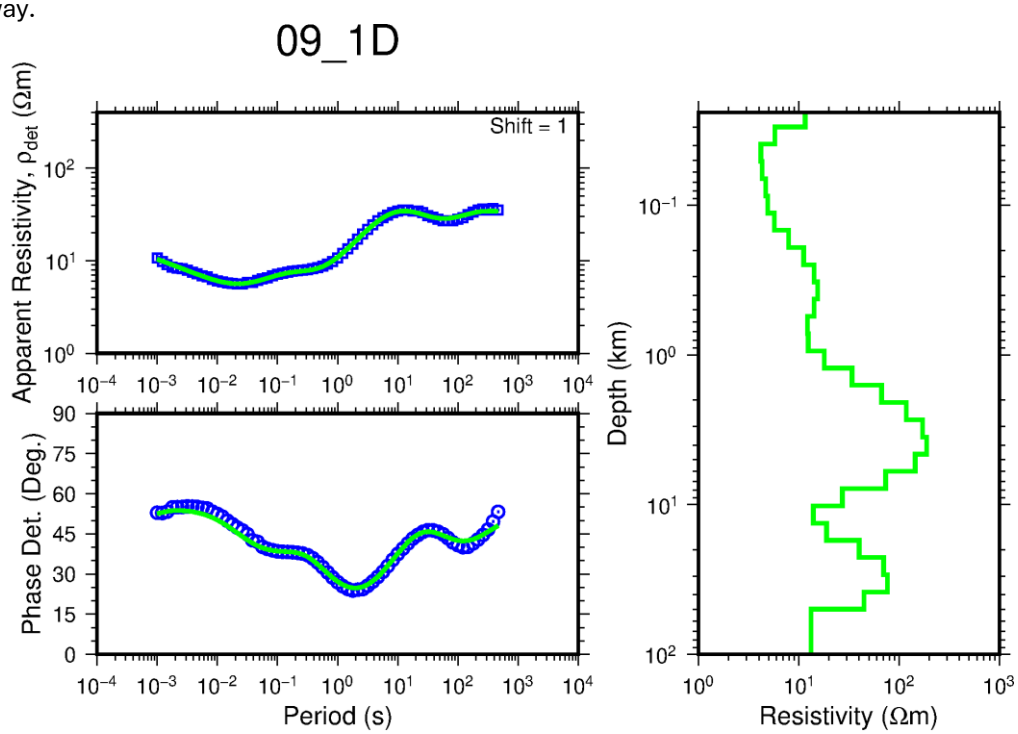


Figure 9. Result of Occam's inversion in sounding 09. On the left, the blue squares and blue circles are the determinant apparent resistivities and phase from the MT data, respectively. On the right, the green curve shows the Occam resistivity model, and the predicted data are the green curves on the left. For this station, the shift multiplier was not used, given a value of 1.

Chave and Jones (2012) described the possible processes which cause static shift: current distortion, topographic effect and electric field or voltage distortion. The use of TEM data co-located with MT soundings corrects these distortions (Pellerin and Hohmann, 1990). But it is important to understand the data as the static shift problem is not always present and not always severe, in some cases corrections may not be necessary or it is just in a few soundings to apply the shift. In geothermal areas the static shift often occurs because of shallow conductive patches that are a result of hydrothermal activity causing alteration in the ground.

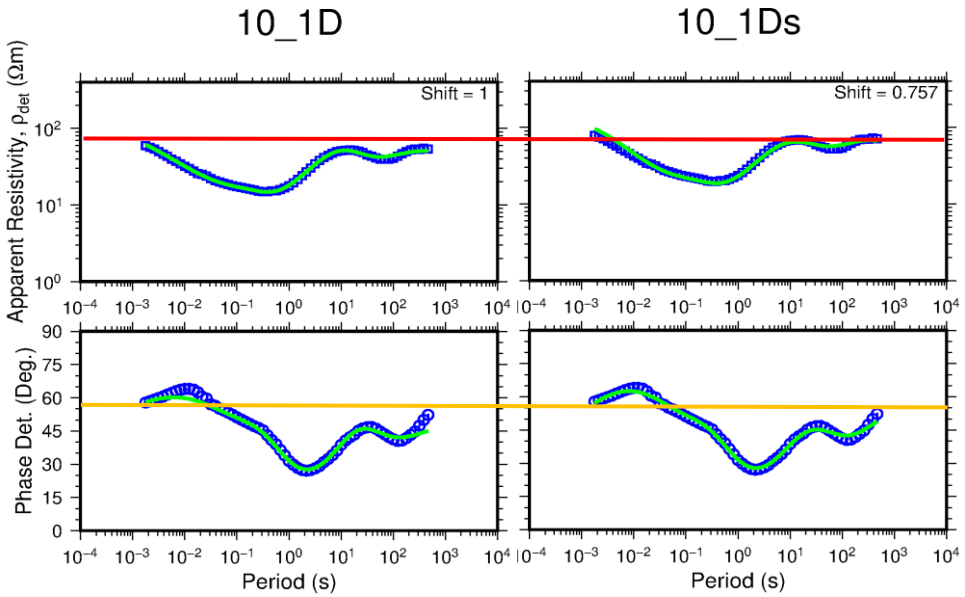


Figure 10. Static shift in sounding 10. The shift is 1 and 0.757 on the left and right, respectively. A shift factor smaller than 1 shifts the apparent resistivity curve up. The red line shows this change. There is no change in the phase as can be seen by the orange line. The green line is the predicted data from a 1D resistivity model (that is now shown) giving a better fit to the phase and apparent resistivity at periods less than 0.01 s. Appendix II in Cahuana, 2023 has the results of the stations were static shift correction was applied.

5 RESULTS

This section is divided into two parts, the first shows the vertical resistivity cross-sections and the second part contains the horizontal resistivity cross-sections maps. Both parts show a few cross-sections, all the cross-sections are displayed in Appendix IV and V in Cahuana (2023).

All vertical and horizontal cross-sections were generated using the programs TEMCROSS and TEMSRESD, respectively. Both programs were written by Eysteinsson (1998) and use the GMT (Generic Mapping Tools) program package.

5.1 VERTICAL RESISTIVITY CROSS-SECTIONS

This part shows resistivity of subsurface to 3 km depth from surface. Figure 14 shows the locations of the five profiles that are shown in the report. Other cross-sections are in Appendix IV in Cahuana (2023).

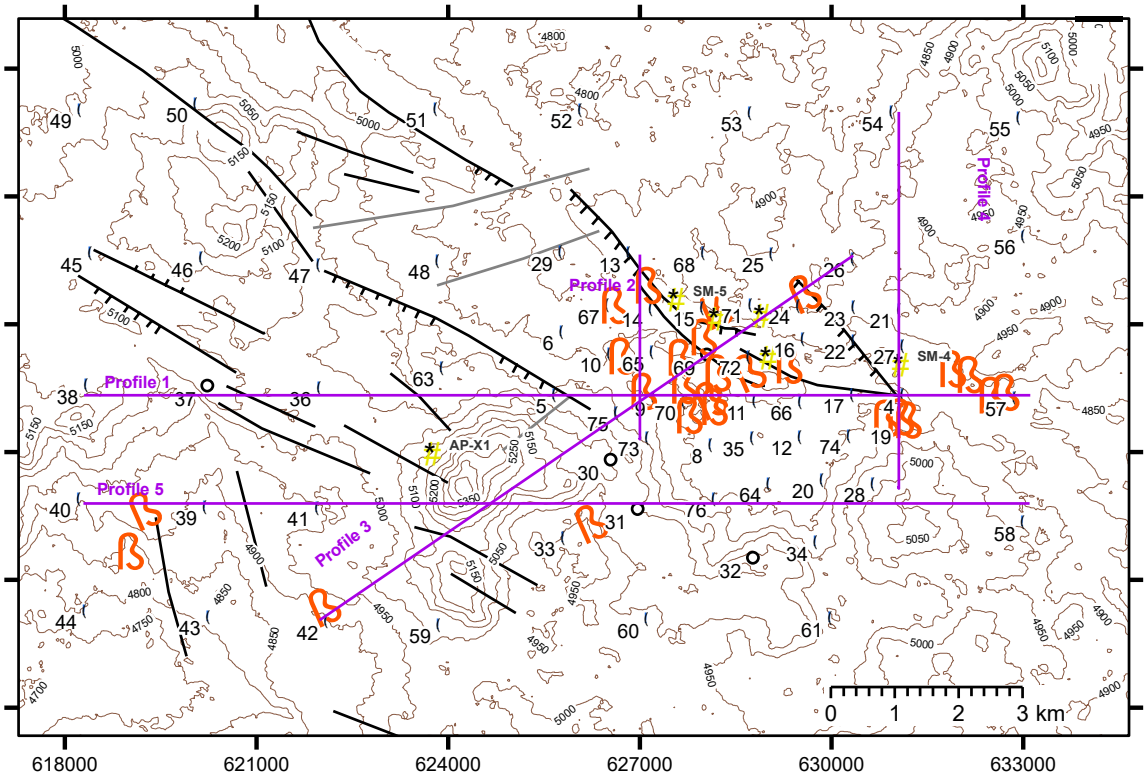


Figure 11. Location of vertical cross-sections are shown as violet lines. Contour lines (brown), faults (black), wells (yellow) and surface manifestations (orange) in the study area. Blue circles are MT stations that where a 1D inversion was performed and white circles are MT stations of bad quality that were not inverted for.

Profile 1 (Figure 12) trends W-E and is close to the wells in Sol de Mañana field. This section displays three layers, the first or upper layer is a high resistivity layer (>100 Ωm) just under the surface which overlies a low resistivity layer or mid layer (<10 Ωm). The third layer is resistive (>70 Ωm) and most probably either the basement or a zone of resistive alteration minerals. Close to soundings 63 and 17-04, the deeper high resistivity layer has an up-doming shape. This is the up-flow zone below the Sol de Mañana field. Between 09 and 70 the middle layer almost rises to the surface. Surface manifestations are reported around soundings 09 and 70 which correlates very well with the low-resistivity cap reaching the surface.

The N-S aligned profile 2 (See Figure 13) shows the low-resistivity cap going close to the surface as in profile 1. The high resistivity layer rises close to the surface. This anomaly is around the wells in SM field.

Profile 3 (See Figure 14) trends SW-NE and has the same three-layered structure as in profiles 1 and 2. The middle layer with lower resistivities is correlated with the argillic zone showen in Figure 4. The middle layer is therefore

the cap rock or the clay cap and reaches 800 meters depth from the surface. Well AP-X1 is located between soundings 42 and 75. It seems that the clay cap extends toward to the SW, but more data are needed to make a further analysis.

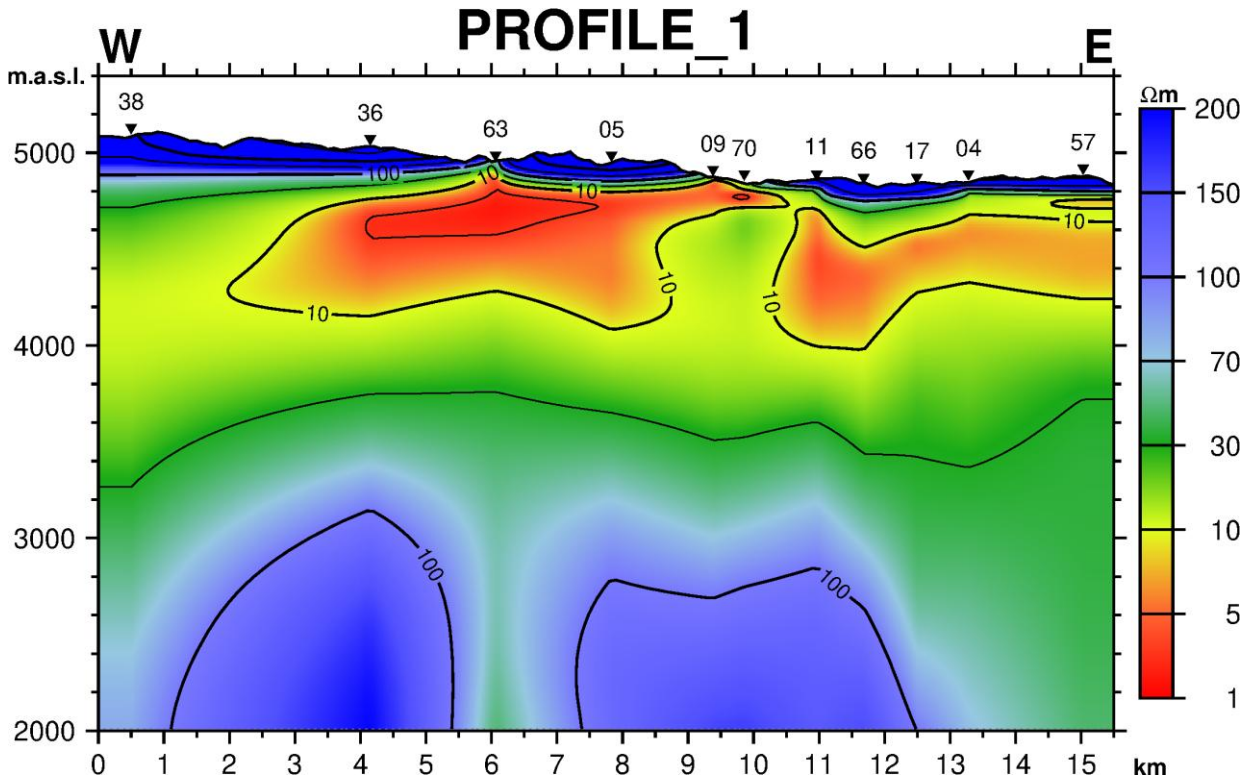


Figure 12. Vertical cross-section along profile 1. Location of profile is shown in Figure 11

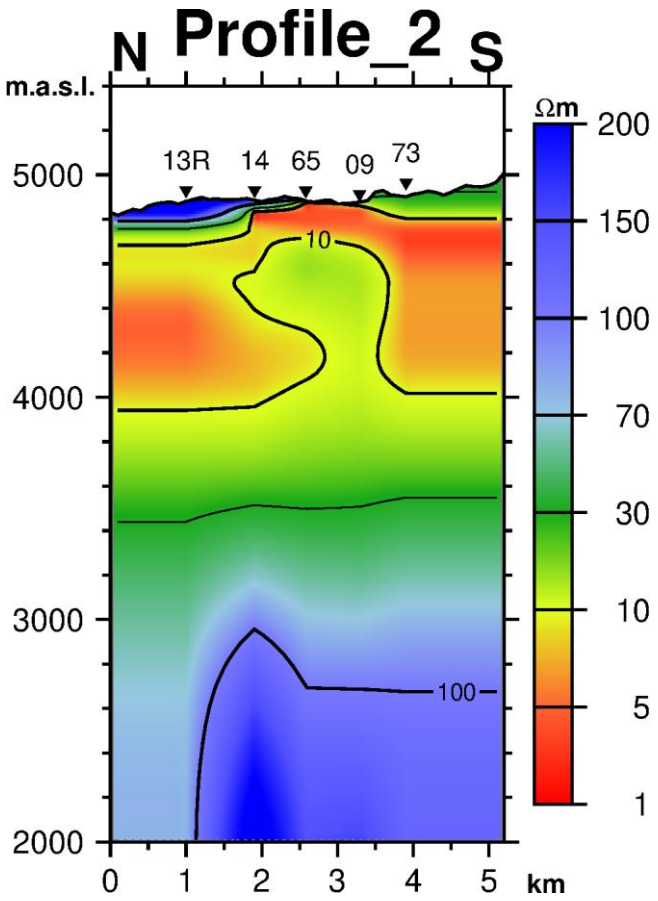


Figure 13. Cross-section along profile 2. Profile location is shown in Figure 11

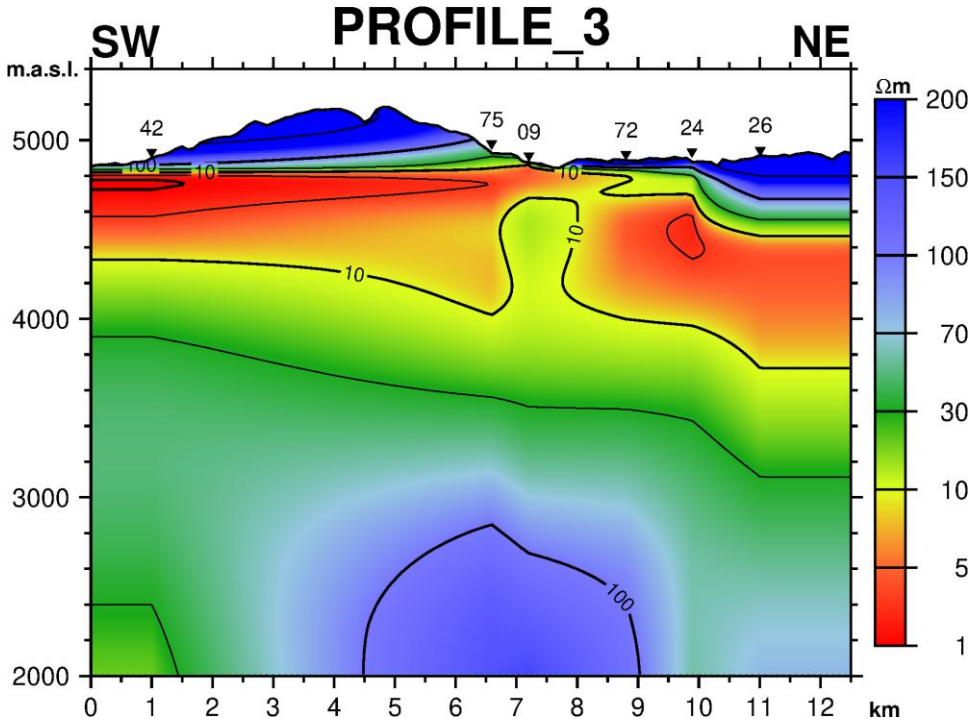


Figure 14. Cross-section along profile 3. Profile location is shown in Figure 11

Profile 4 is oriented N-S and shows the deep resistive layer rising close to the surface around soundings 04 and 19. This feature correlates with a NW-SE fault, mapped on the surface (Figure 6). This fault seems to be permeable surface manifestations were reported east of soundings 19 and 28 in recent years.

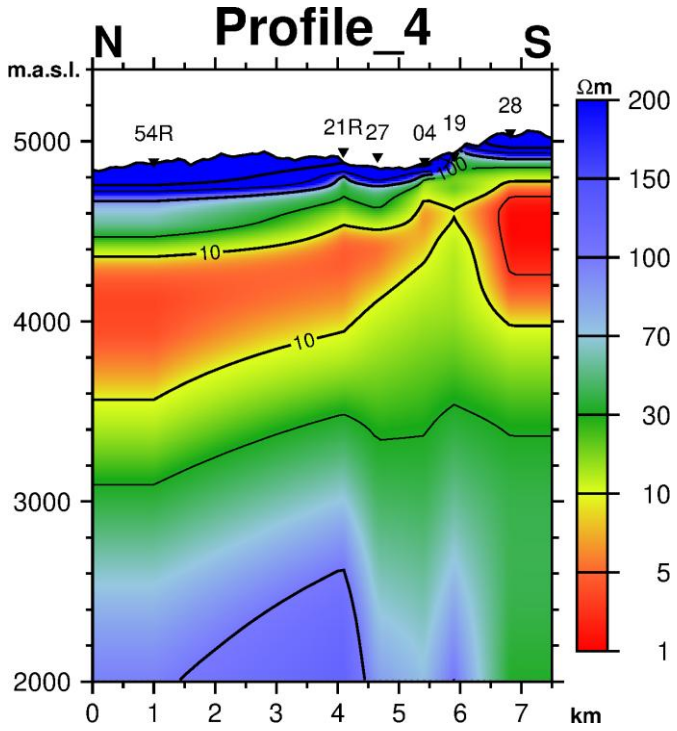


Figure 15. Cross-section along profile 4. Profile location is shown in Figure 11

Profile 5 is oriented W-E. Underneath sounding 41 a remarkable updoming feature is observed. A silicified alteration zone at 500 m to 1000 m depth is present in well AP-1 which corresponds to the resistive core under sounding 41. The temperature in AP-1 well at this depth interval isb between 185 - 225 °C. SW of sounding 41 geothermal manifestations have been reported (Pereyra, 2023).

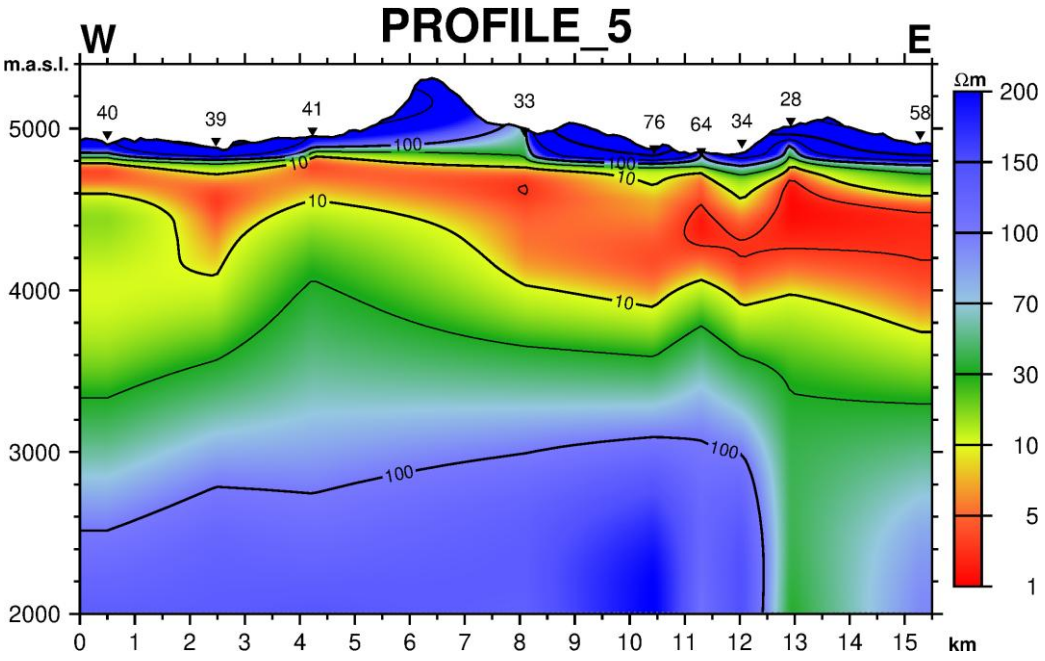


Figure 16. Cross-section along profile 5. Profile location is shown in Figure 11

5.2 HORIZONTAL RESISTIVITY CROSS-SECTIONS

This part shows resistivity of subsurface at different depths. Detailed horizontal cross-sections are in Appendix V in Cahuana (2023).

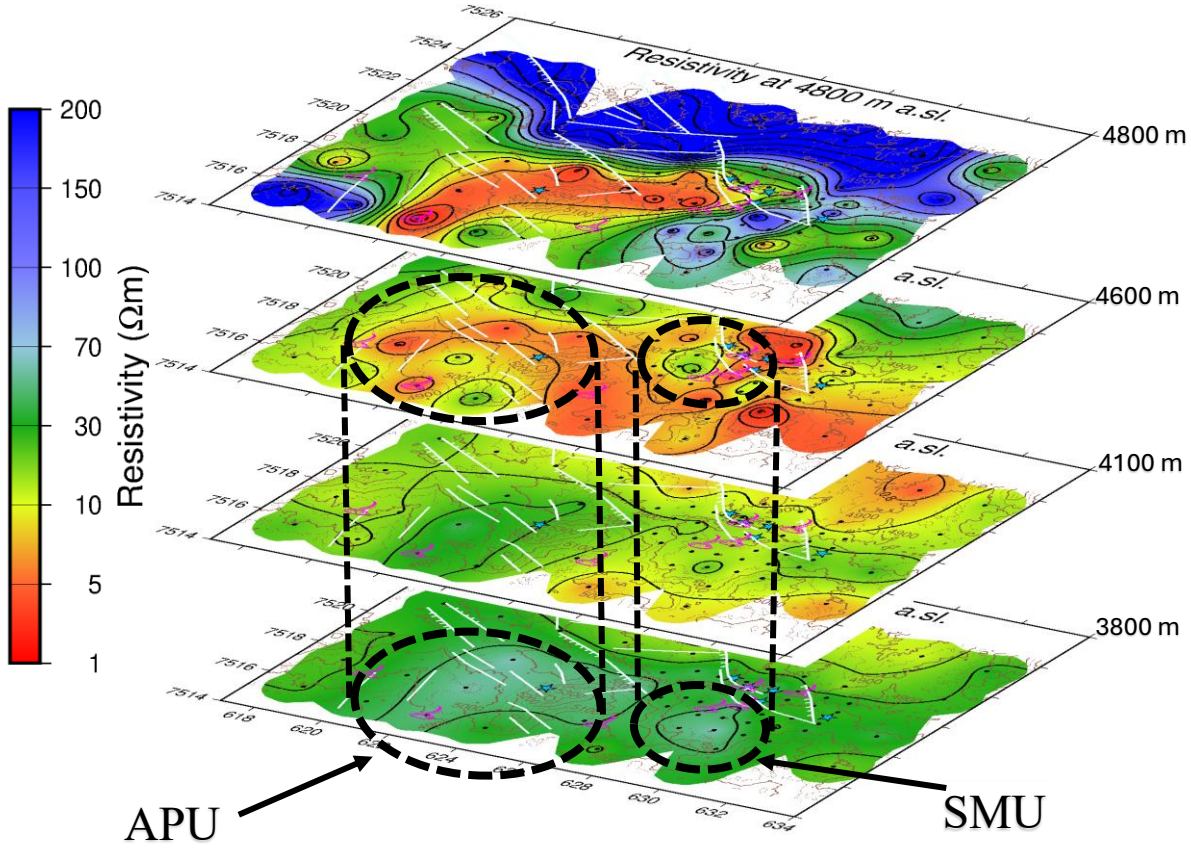


Figure 17. Horizontal cross-section through the 1D resistivity model at 4800 m.a.s.l., 4600 m.a.s.l., 4100 m.a.s.l. and 3800 m.a.s.l. Black points are MT soundings, white lines are faults and purple icons are fumaroles. Black dashed line is the upflow zones.

Figure 17 shows the resistivity at 4800 m.a.s.l., 4600 m.a.s.l., 4100 m.a.s.l. and 3800 m.a.s.l. At 4800 m.a.s.l. the low-resistivity layer is trending in NE-SW direction, beginning close to the wells in SM field, crossing the location of well AP-1, and farther SW. At 4600 m a high resistivity anomaly appears in the center, just west of the SM wells, and growing larger with increasing depth. Similar resistive anomaly is seen to the southwest below the AP-X1 well. These high-resistivity anomaly could be an up-flow zones. These anomalies are called for this paper as Sol de Mañana upflow (SMU) and Apacheta upflow (APU).

At 4100 m.a.s.l. a low-resistivity layer appears with a trend in NE direction. A big uncertainty is associated with it as not many soundings are located there. At 3800 m.a.s.l the survey area is generally becoming more resistive, with two high resistivity anomalies where the possible reservoirs are located (see black dashed lines in Figure 17).
Six soundings were corrected for static shift during the 1D inversion. This is important to keep in mind because the correction might influence the shape of the two up-doming anomalies, SMU and APU.

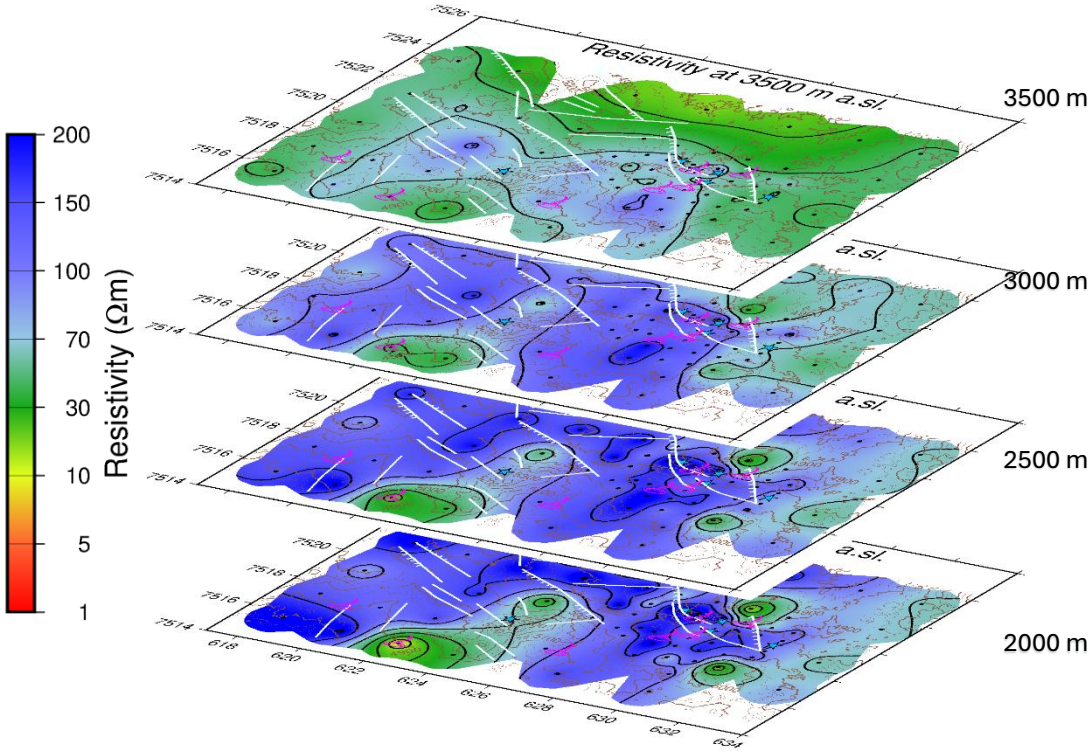


Figure 18. Horizontal cross-sections through the 1D resistivity model at 3500 m.a.s.l., 3000 m.a.s.l., 2500 m.a.s.l. and 2000 m.a.s.l. Black points are MT soundings, white lines are faults and purple icons are fumaroles.

Figure 18 shows the resistivity at 3500 m.a.s.l., 3000 m.a.s.l., 2500 m.a.s.l. and 2000 m.a.s.l. The shallow conductive layer (<10 Ωm) is not present at these depths and the high resistivity core is becoming more resistive in the center and in the southwest at 3500 m.a.s.l. and 3000 m.a.s.l., surrounded by a moderate anomaly (10 Ωm -60 Ωm), plausibly representing the bottom patches of the clay rich formations.

5.3 COMPARISON BETWEEN ALTERATION MINERALOGY AND RESISTIVITY MODEL

The alteration minerology is shown in Figure 6. The vertical cross-section shown in Figure 12 shows profile 1 (location shown in Figure 11), which is closest to the SM wells. It seems that the argillic and silicified zones in the wells correspond to the clay cap. The clay cap starts at a 0-100 m depth and extends down to roughly 700-1000 m below the surface. This correlates very well with the depth of the bottom of the silicified zone in the wells.

5.4 CONCLUSIONS AND RECOMMENDATIONS

The conclusions and recommendations that have come from this report are as follows:

- A low-resistivity layer is observed in the results of the 1D inversion of the MT data. The layer is interpreted to be the cap rock in Sol de Mañana field and Apacheta field. The lower resistivity layer reaches 800 m depth below the surface and correlates with the argillic and silicified zones in the wells in Sol de Mañana and Apacheta fields.
- Two upflow zones are identified as up-doming anomalies in the 1D resistivity model, the SMU and APU anomalies. It is not possible to identify if these zones are connected.
- A denser study in the SW and E of Laguna Colorada area will help to understand the conductive anomalies in SMU and APU.
- The static shift must be studied further because it is can greatly influence the results of the 1D inversion. It is unknown how much the static shift problem is present in Sol de Mañana and Apacheta fields and it is therefore recommended to carry out a TEM survey where MT data exist.

ACKNOWLEDGEMENTS

Cahuana O.

Thank you, God, for your blessings. Thanks to my parents Daniel and Elizabeth, because without their support I could not have been part of this training, their love and teachings are the most important tools I have in my life. I am always growing in my knowledge because my parents permanently inspired me to be a better person and to be a better professional. To my brother Ronald and his family (Ibeth, Jaime, Lorena) an inspiration for their love to me. I want to teach all these things to my children, Piero and Leandro, because they are my inspiration to be better every day.

REFERENCES

Aguilera, F., Apaza, F., del Carpio, J., Grosse, P., Jiménez, N., Ureta, G., Inostroza, M., Báez, W., Layana, S., González, C., Rivera, M., Ortega, M., González, R., and Iriarte, R., 2021: Advances in scientific understanding of the Central Volcanic Zone of the Andes: a review of contributing factors. Bulletin of Volcanology, Vol. 84.

Aliaga, R.; 1985: Geothermal Potential in Bolivia. 6th New Zealand Geothermal Workshop 1984, 225-226.

Andrews, S., 2023: Electromagnetic Waves. In: Light and Waves. Springer, Cham, pp. 273 – 305.

Árnason, K., 1989: Central loop transient electromagnetic sounding over a horizontally layered earth. Orkustofnun, Reykjavík, report OS-89032/JHD-06, 129 pp.

Árnason, K., 2006b: TEMTD, a programme for 1D inversion of central-loop TEM and MT data. Short manual. ÍSOR – Iceland GeoSurvey, Reykjavík, manual, 17 pp.

Árnason, K., Eysteinsson, H., Hersir, G.P., 2010: Joint 1D inversion of TEM and MT data and 3D inversion of MT data in the Hengill area, SW Iceland. Geothermics, Vol 39, 13-34.

Árnason, K., 2015: The static shift problem in MT soundings. Proceedings of the World Geothermal Congress 2015, Melbourne, Australia, 12 pp.

Árnason, K., 2020: New Conceptual Model for the Magma-Hydrotermal-Tectonic System of Krafla, NE Iceland. Geosciences, Vol. 10, Issue 1, 27 pp.

Battocletti, L., Lawrence, R., 1999. Database of Geothermal Resources in Latin American & the Caribbean. Report for Sandia National Laboratories, Contract No. AS-0989, Bob Lawrence & Associates Inc.

Bahr, K., 1991: Geological noise in magnetotelluric data: a classification of distortion types, Physics of the Earth and Planetary Interiors, Vol. 66, p. 24-38.

BEN, 2022: National Energy Balance (Balance Energético Nacional) 2006 – 2021. Ministerio de Hidrocarburos y Energía del Estado Plurinacional de Bolivia.

Bird, D., Schiffman, P., Elders, W., and Williams, E., 1983: Calc-silicate mineralization in active geothermal systems. Stanford, California, United States.

Brasse, H., Lezaeta, P., Rath, V., Schwalenberg, K., Soyer, W., Haak, V., 2002: The Bolivian Altiplano Conductivity Anomaly, Journal of Geophysical Research Atmospheres, Vol. 107, Issue B5, pp. EPM 4-1-EPM 4-14.

Browne, P., Ellis, A., 1970: The Ohaki-Broadlands hydrothermal area, New Zealand; mineralogy and related geochemistry. American Journal of Science, Vol. 269, pp. 97–131.

Browne, P., 1978: Hydrothermal Alteration in Active Geothermal Fields. Annual Review of Earth and Planetary Sciences, Vol. 6, pp. 229–248.

CFE, 1997: Potential certification of Sol de Mañana geothermal field. Comisión Federal de Electricidad (CFE), internal report submitted to ENDE (in Spanish), 225 pp.

Chave, A.D., and Jones, A.G., 2012: The Magnetotelluric Method: Theory and Practice, Cambridge University Press, Cambridge, 552 pp.

Corneau, M.; 2015: Electrical Resistivity Structure of the Altiplano-Puna Magma Body and Volcan Uturuncu from Magnetotelluric Data, Department of Physics, University of Alberta, 337 pp.

Carrasco, R.; 1976: Preliminary Report on Bolivia's Geothermal Resources, Second United Nations Symposium on the Development and Use of Geothermal Resources, Report 09 in: Volume 1, Section I - Present Status of Resources Development, 1009 pp.

Constable, S.C., Parker R.L., Constable, C.G., 1987: Occam's inversion: A practical algorithm for generating smooth models from EM sounding data, Geophysics, Vol. 52, pp. 289-300.

Corrado, L. Aldega, A.S. Celano, A.A. De Benedetti, and G. Giordano, 2014: Cap rock efficiency and fluid circulation of natural hydrothermal systems by means of XRD on clay minerals (Sutri, Northern Latium, Italy). Geothermics, Vol. 50, pp. 180-188.

Christopherson, K., 2022: Mapping sub-basalt structure of the Columbia River Basin with MT. MTNet EMinar. Website: https://www.youtube.com/watch?v=c1lllFynFIs

DeSilva, S.L., 1989: Altiplano-Puna volcanic complex of the Central Andes, Geology, Vol. 17, pp. 1102–1106.

DeSilva, S., Francis, P.W., 1991: Volcanoes of the Central Andes. Geological Magazine, Vol. VIII, 216 pp.

Delgadillo, Z.; 2000: State of The Geothermal Resources in Bolivia, World Geothermal Congress 2000, Japan.

Donovan, P. T.; 1984: The Status of High Enthalpy Geothermal Exploration in the Developing Countries. Geothermics, Vol. 14, Issues 2/3, pp. 487-494.

ENEL, 1986: Geothermal feasibility study in Laguna Colorada area. ENEL, internal report submitted to ENDE (in Spanish), 93 pp.

ENDE, 2017: Pre-investment technical design study for 100 MW Construction of Geothermal Plant in Laguna Colorada Project, internal report of ENDE (in Spanish), 243 pp.

Eysteinsson, H., 1998: TEMRESD, TEMMAP and TEMCROSS plotting programs. ÍSOR – Iceland GeoSurvey, unpublished programs, and manuals.

Flóvenz, Ó.G., Spangenberg, E., Kulenkampff, J., Árnason, K., Karlsdóttir, R. and Huenges E., 2005: The role of electrical conduction in geothermal exploration. Proceedings World Geothermal Congress 2005, Antalya, Turkey, CD, 9 pp.

Gamble, T.D., Goubau, W.M., and Clarke, J., 1979: Magnetotellurics with a remote magnetic reference. Geophysics, Vol. 44, Issue 1, pp. 53-68.

Gawell, K., Reed, M., and Wright, M., 1999: Preliminary Report: Geothermal Energy, The Potential for Clean Power from the Earth. Geothermal Energy Association.

Griffiths, D.J., 2013: Introduction to Electrodynamics, 4th Edition, Prentice Hall, 623 pp.

GRG, 2015: Apacheta 1 (AP-1) – Flow Test Report. Geothermal Resource Group, Inc., internal report submitted to ENDE (in Spanish), 10 pp.

Haffen, S., Diraison, M., Corsini, M. and Géraud, Y., 2021: Geological Model and Fluid Flow Pathways of the Sol de Mañana/Apacheta Geothermal Field (Altiplano – Bolivia). World Geothermal Congress 2021, Iceland.

Hersir, G.P., Árnason, K., 2015: Resistivity of rocks. Presented at "Short Course X on Exploration for Geothermal Resources", organized by UNU-GTP, GDC and KenGen, at Lake Bogoria and Lake Naivasha, Kenya.

Hersir, G.P., Guðnason, E.A., Flóvenz O.G.; 2022: Geophysical Exploration Techniques. In: Letcher, Trevor M., Comprehensive Renewable Energy, 2nd edition, Vol. 7, Elsevier, pp. 26–79.

JETRO, 2008: Study of feasibility for construction of the Laguna Colorada geothermal plant Potosi, Bolivia. Japan External Trade Organization (JETRO), internal report submitted to ENDE (in Spanish), 269 pp.

INE, 2021: Bolivia: Electrical power generation, per source, 2012 – 2021. Statistics National Institute (in Spanish).

JICA, 2013: Project preparation for the Project Construction of Laguna Colorada geothermal plant. Japan International Cooperation Agency (JICA), internal report submitted to ENDE (in Spanish), 185 pp.

Jones, A., 1988: Static shift of MT data and its removal in a sedimentary basin environment. Geophysics, Vol. 53, pp. 967-978.

Jones, A.G., and Groom, R.W., 1993, Strike-angle determination from the magnetotelluric impedance tensor in the presence of noise and local distortion: rotate at your peril!. Geophysical Journal International, Volume 113, Issue 2, pp. 524–534.

Kahwa, E.; 2015: Geophysical Exploration of High Temperature Geothermal Areas using Resistivity Methods. Case Study: Theistareykir Area, NE Iceland, World Geothermal Congress 2015, Australia.

Kearey, P., Brooks, M., Hill, I., 2002: An Introduction to Geophysical Exploration, Third Edition. Blackwell Science, 281 pp.

Lagat, J., 2013: Hydrothermal Alteration Mineralogy in Geothermal Fields with case examples from Olkaria Domes Geothermal Field, Kenya. Presented at “Short Course VIII on Exploration for Geothermal Resources”, organized by UNU-GTP, GDC and KenGen, Naivasha, Kenya.

Maffucci, R., Corrado, S., Aldega, L., Bigi, S., Chiodi, A., di Paolo, L. Giordano, G., and Invernizzi, C., 2016: Cap rock efficiency of geothermal systems in fold-and-thrust belts: Evidence from paleo-thermal and structural analyses in Rosario de La Frontera geothermal area (NW Argentina). Journal of Volcanology and Geothermal Research, Vol. 328, pp. 84-95.

Palacky, G. J., 1988: Resistivity Characteristics of Geologic Targets. In: Nabighian, M., Electromagnetic Methods in Applied Geophysics, Vol. 2, pp. 53-129.

Park, S.K., Livelybrooks D.W., 1989: Quantitative interpretation of rotationally invariant parameters in magnetotellurics. Geophysics, Volumen 54, Issue 11, pp. 1483-1490.

Parkinson, W.D., 1959: Directions of rapid geomagnetic fluctuations, Geophysical Journal of the Royal Astronomical Society, Vol. 2, Issue 1, pp. 1-14.

Pellerin, L., and Hohmann, G., 1990: Transient electromagnetic inversion: A remedy for magnetotelluric static shifts. Geophysics, Vol. 55, Issue 9, pp. 1242-1250.

Peña, J., 2020: Exploring low-carbon development pathways for Bolivia – A model based analysis focused on the energy sector, Department of Energy and Environmental Systems, Royal Institute of Technology, 171 pp.

Pereyra, B., Meneses, E., Kapinos, G., and Brasse H., 2023: Three-dimensional magnetotelluric inversion for the characterization of the Sol de Mañana high-enthalpy geothermal field, Geothermics, Volume 113, 102748.

Piscaglia, F., 2012: The High Temperature Geothermal Field of the Apacheta-Aguilucho Volcanic Complex (Northern Chile): Geo-Petrographic Surface Exploration, Crustal Heat Sources and Cap-Rocks. Plinius, Vol. 38.

PDES, 2020: Social and Economical Developing Plan 2021-2025: Rebuilding the Economy to live well, towards industrialization with import substitution (in spanish). Ministry of Development Planning of the Plurinational State of Bolivia.

PLUTONS, 2010: Probing Lazufre and Uturuncu TOgether: Nsf (USA), Nerc (UK), Nserc (Canada), Sergeotecmin (Bolivia), Sernageomin (Chile), Observatorio San Calixto (Bolivia), Universidad Nacional de Salta (Argentina), Universidad Mayor San Andres (Bolivia), Universidad de PotoSi (Bolivia), Sernap (Bolivia), Chilean

Seismological Service, Universidad de San Juan (Argentina), https://plutons.science.oregonstate.edu/about/.

Salas, H., 2014: Origin of the Roboré, Charagua and Camiri hot springs. Bolivia Tecnociencia Universitaria (in Spanish).

Santos, L., Taleghani A., Elsworth D., 2022: Repurposing abandoned wells for geothermal energy: Current status and future prospects. Renewable Energy, Volume 194, 2022, pp. 1288-1302,

Shalivahan, and Bimalendu, B., 2002: How remote can the far remote reference site for magnetotelluric measurements be?. Journal of Geophysical Research, Vol. 107, Issue B6.

Simpson, F., and Bahr, K., 2005: Practical magnetotellurics. Cambridge University Press, Cambridge, UK, 254 pp.

Swift, C.M., 1967: A magnetotelluric investigation of an Electrical Conductivity Anomaly in the Southwestern United States, MIT, PhD thesis.

Unsworth, M., Rondenay, S., 2013: Mapping the distribution of fluids in the crust and lithospheric mantle utilizing geophysical methods. In: Metasomatism and the Chemical Transformation of Rock. Springer, pp. 535-598.

Urzua, L., Powell, T., Cumming, W., Dobson, P., 2002: Apacheta, a New Geothermal Prospect in Northern Chile. Transactions – Geothermal Resources Council 26.

Tozer, B., Sandwell, D., Smith, W., Olson, C., Beale, J., and Wessel, P., 2019: Global Bathymetry and Topography at 15 Arc Sec: SRTM15+. Earth and Space Science, Vol. 6, Issue 10, pp. 1847 – 1864.

Villarroel, D., 2014: Geochemical studies of geothermal fluid and evaluation of well test results from wells SM-01, SM-02 and SM-03, Sol de Mañana field, geothermal project, Laguna Colorada, Bolivia. Report 32 in: Geothermal training in Iceland 2014. UNU-GTP, Iceland, 697-720 pp.

Waring, G.A.; 1965: Thermal Springs of the United States and Other Countries of the World – A Summary. Washington, U.S. Govt. Print. Off., 392 pp.

West JEC, 2010: Preparatory study for the geothermal development of Sol de Mañana, Bolivia. West Japan Engineering Consultants, Inc. (West JEC), internal report (in Spanish), submitted to ENDE, Bolivia.

West JEC, 2008: Feasibility study for the geothermal power plant construction on Laguna Colorada. West Japan Engineering Consultants, Inc. (West JEC), internal report (in Spanish), submitted to ENDE, Bolivia.

West JEC, 2013: Preparatory Project for the Project Construction of the Geothermal Laguna Colorada Power Plant. West Japan Engineering Consultants, Inc. (West JEC), internal report (in Spanish), submitted to ENDE, Bolivia.